Articles in PresS. Am J Physiol Endocrinol Metab (June 21, 2011). doi:10.1152/ajpendo.00709.2010

NOD1 activation induces proinflammatory gene expression and insulin resistance in 3T3-L1 adipocytes

Ling Zhao[1,3,4], Pan Hu[1], Yijun Zhou[1], Jaanki Purohit[1], Daniel Hwang[2,4]

[1]Department of Nutrition, The University of Tennessee, Knoxville, Tennessee; [2]Western Human Nutrition Research Center, United States Department of Agriculture and Department of Nutrition, University of California, Davis, California.

Running title: NOD1 activation leads to insulin resistance

[3] Correspondence author: Dr. Ling Zhao, Department of Nutrition, The University of Tennessee, 1215 W. Cumberland Ave, Knoxville, Tennessee. Phone: (865)974-1833, Fax: (865)974-3491, E-mail: ling.zhao@utk.edu.

[4] Dr. Ling Zhao and Dr. Daniel Hwang share the senior authorship.

Abbreviations

iE-DAP, γ-D-Glu-meso-diaminopimelic acid; FFA, free fatty acid; GSK, glycogen synthase kinase; IKK, IkappaB kinase; IRS-1, Insulin receptor substrate 1; JNK, c-Jun N-terminal kinase; IL-6, interleukin 6; IL-8, interleukin 8; LPS, lipopolysaccharide; LRR, leucine-rich repeat; MAPK, mitogen-activated protein kinase; MCP-1, monocyte chemotactic protein 1; MDP, muramyl dipeptide; MIP-2, macrophage inflammatory protein 2; NF-κB, nuclear factor kappa B; NOD, nucleotide-binding oligomerization domain containing protein; PAMP, pathogen-associated molecular patterns; PRR, pattern recognition receptor; RANTES, Regulated upon Activation, Normal T-cell Expressed, and Secreted; SFA, saturated fatty acid; TLR, Toll-like receptor; TNF-α, tumor necrosis factor α; Tri-DAP, L-Ala-γ-D-Glu-meso-diaminopimelic acid.

Abstract

Chronic inflammation is associated with obesity and insulin resistance. However, the underlying mechanisms are not fully understood. Pattern recognition receptors Toll-like receptors and Nucleotide-oligomerization domain containing proteins play critical roles in innate immune response. Here we report that activation of nucleotide binding oligomerization domain containing protein 1 (NOD1) in adipocytes induces proinflammatory response and impairs insulin signaling and insulin-induced glucose uptake. NOD1 and NOD2 mRNA are markedly increased in differentiated murine 3T3-L1 adipocytes and human primary adipocyte culture upon adipocyte conversion. Moreover, NOD1 mRNA is markedly increased only in the fat tissues in diet-induced obese mice, but not in genetically obese *ob/ob* mice. Stimulation of NOD1 with a synthetic ligand Tri-DAP induces proinflammatory chemokine MCP-1, RANTES and cytokine TNF-α and MIP-2 (human IL-8 homolog) and IL-6 mRNA expression in 3T3-L1 adipocytes in a time and dose dependent manner. Similar proinflammatory profiles are observed in human primary adipocyte culture stimulated with Tri-DAP. Furthermore, NOD1 activation suppresses insulin signaling as revealed by attenuated tyrosine phosphorylation, and increased inhibitory serine phosphorylation, of insulin receptor substrate-1and attenuated phosphorylation of Akt and downstream target GSK3α/3β, resulting in decreased insulin-induced glucose uptake in 3T3-L1 adipocytes. Together, our results suggest that NOD1 may play an important role in adipose inflammation and insulin resistance in diet-induced obesity.

Key Words: NOD1, Tri-DAP, inflammation, insulin resistance, 3T3-L1

Introduction

Obesity is becoming a global epidemic that affects both adults and children. Accumulating evidence indicates that obesity is associated with chronic inflammation, as characterized by macrophage infiltration into adipose tissue and elevated proinflammatory chemokine/cytokine secretion (43, 44, 47). Chronic inflammation in adipose tissue is causally linked to obesity associated insulin resistance, type 2 diabetes and other metabolic dysfunctions (10, 33). Innate immune receptors play critical roles in innate immune responses and inflammation. Innate immune receptors are pattern recognition receptors (PRR) that recognize the pathogen associated molecular patterns (PAMPs) on invading pathogens, and activate downstream signaling pathways leading to the up-regulation of diverse arrays of proinflammatory gene expression for tailored immune responses. Two prominent families are membrane-bound Toll-like receptors (TLRs) and cytosolic Nucleotide oligomerization domain-like receptors (NLRs) (40).

TLRs are transmembrane receptors composed of extracellular leucine-rich repeat (LRR) motifs, and a cytoplasmic Toll/interleukin-1 receptor (TIR) homology domain. So far, 10 and 12 functional TLRs have been identified in humans and mice, respectively (20). The respective bacterial or viral PAMPs that individual TLR detects have been well characterized (40). Recent evidence has shown TLR4 and TLR2 might be activated by non-microbial, endogenous molecules (e.g., saturated fatty acids) in inducing “sterile inflammation” (27). We and others have shown that TLR4 and TLR2 (dimerized with TLR6 or TLR1) can mediate saturated fatty acid (SFA)-induced NF-κB activation and target gene response in murine macrophage RAW264.7 cells (26, 28) and myotubes C2C12 cells (35), respectively. These studies were

followed by the investigations of TLRs in 3T3-L1 adipocytes and in vivo in TLR4 or TLR2 knockout mice. SFA-induced TNF-α and IL-6 gene expression were blunted in TLR4-knockdown or TLR4-knockout (TLR4-/-) adipocytes (36). TLR4 knockout mice and C3H/HeJ mice, which carry a spontaneous mutation inactivating *Tlr4*, were protected against adipose inflammation and the development of insulin resistance in response to a systemic lipid infusion or a high fat diet, respectively (30, 36, 39). Mice lacking TLR2 were protected from insulin resistance, macrophage infiltration and adiposity induced by two dietary models that approximate contemporary diet compositions (15). Moreover, mice with TLR2 deficiency were also protected from high fat diet-induced insulin resistance, tissue inflammation and pancreatic β cell dysfunction (6). Consistent with these results, a broad mRNA expression profile of TLRs and their functionalities have been demonstrated in mature 3T3-L1 adipocytes (25) and human primary adipocytes isolated from fat tissue (24).

NLRs are a family of cytosolic sensors that play important roles in innate immunity and inflammation. These NLRs display a central nucleotide-binding domain, an N-terminal protein interaction domain, and a C-terminal leucine-rich repeat (LRR) domain (8). Two prominent members of NLRs are NOD1 and NOD2, whose recognition motifs in bacterial peptidoglycan have been mapped. The minimal peptidoglycan structure that NOD1 recognizes is a dipeptide, γ-D-Glu-meso-diaminopimelic acid (iE-DAP) (4) or a tripeptide, L-Ala-γ-D-Glu-meso-diaminopimelic acid (Tri-DAP) (12) derived mostly from Gram-negative bacteria, whereas NOD2 recognizes the minimal peptidoglycan muramyl dipeptide, MurNAc-L-Ala-D-isoGln (MDP), from both Gram-positive and Gram-negative bacteria (13, 17). Similar to TLR, NOD

activation leads to the activation of signaling pathways including NF-κB and MAPK, leading to proinflammatory gene expression (9, 16).

We have studied the role of NOD1 and NOD2 in SFA-induced inflammation (49). In human intestinal epithelial HCT116 cells, which express abundant NOD1 and NOD2, but no detectable levels of TLR4 and TLR2, and in reconstituted 293T cells transfected with NOD expression plasmid, both NOD1 and NOD2 can mediate SFA-induced NF-κB activation and target gene IL-8 expression (49). However, the roles of NOD proteins on adipose inflammation and insulin resistance have not been studied.

Therefore, we investigated the potential roles of NOD proteins in inducing inflammation in adipocytes, leading to obesity associated insulin resistance. Here we report that both NOD1 and NOD2 mRNA are markedly up-regulated during adipocyte conversion of murine 3T3-L1 cells and human primary adipocyte culture. NOD1 mRNA is markedly increased only in the fat tissues in diet-induced obese mice, but not in genetically obese *ob/ob* mice. Moreover, stimulation of NOD1 with the synthetic ligand induces proinflammatory gene expression, suppresses insulin signaling and subsequent glucose uptake in 3T3-L1 adipocytes.

Materials and methods

Reagents

NOD1 synthetic ligand Tri-DAP and iE-DAP were purchased from invivoGen (San Diego, CA). Lipopolysaccharide (LPS), saturated free fatty acids, methylisobutylxanthine, dexamethasone and insulin were purchased from Sigma (St. Louis, MO). Pharmacological inhibitors Caffeic acid phenethyl ester, Bay117821, SB203580, SP600125, PD98054 were from Tocris bioscience (Ellisville, MI). Antibodies anti-phospho-Akt (Ser473), anti-phospho-Akt (Thr308), anti-Akt, anti-phospho-GSK3α/3β, anti-phospho-ERK1/2 (Thr202/Tyr204), anti-ERK1/2, anti-phospho-p38(Thr180/Tyr182), anti-p38, anti-phospho-JNK(Thr183/Tyr185), anti-JNK, anti-phospho-p65(Ser536), anti-p65 and anti-phospho-IκBα(Ser32), anti-Insulin receptor substrate 1(IRS-1), anti-phospho-IRS-1(Ser612), anti-phospho-IRS-1(Ser307) were purchased from Cell signaling Technology, Inc. (Danvers, MA). Antibodies anti-phospho-IRS-1 (Tyr632) and anti-phospho-Tyrosine (PY99) were from Santa Cruz biotechnology, Inc. (Santa Cruz, CA). Antibody anti-phospho-Tyrosine (4G10) was from Millipore (Billerica, MA). Anti-β-actin and anti-tubulin antibodies were purchased from Sigma.

Animals

Diet-induced obese (DIO) mice as well as *ob/ob* and their control mice were purchased from the Jackson Laboratory. For DIO mice, male C57BL/6J mice were fed with high-fat diet (60% Kcal% from fat, Research Diets Inc.) or regular chow diet for 20 weeks before sacrificed at 26 weeks of age. Male *ob/ob* and their control mice were fed with chow diet for 8 weeks before sacrificed at 14 weeks of age. The mice studies were approved by the Institutional Animal Care and Use Committee at the University of Tennessee.

146

147 *Adipocyte differentiation*

148 Murine 3T3-L1 fibroblasts (ATCC, Manassas, VA) were grown in Dulbecco's modified
149 Eagle's medium (DMEM) containing 10% calf serum (Hyclone) in 5% CO2, 37^0C environment
150 until they reach confluence. The differentiation was initiated as described (29). Briefly, on the
151 day the cells reach confluence (designated as day 0, D0), cells were treated with differentiation
152 DMEM containing 10% Fetal bovine serum (FBS, Atlas biologicals), 10µg/mL insulin, 1µM
153 dexamethasone, and 0.5mM 3-isobutyl-1-methylxanthine for 3 days. The cells were then grown
154 in maintenance DMEM containing 10% FBS and 10µg/mL insulin for additional two more days
155 followed by in DMEM containing 10% FBS until the cells were used for NOD1 stimulation
156 experiments. Typically, adipocyte conversion occurred in 99% of the cells 8 days post the
157 initiation of differentiation (D8). Human subcutaneous fat derived primary preadipocytes culture
158 was purchased from Zen-bio (Research Triangle Park, NC) and were grown and differentiated
159 according to the manufacturer's instructions. Briefly, human primary preadipocytes were seeded
160 and grown in 60mm tissue culture dishes in preadipocyte medium until confluence. The
161 differentiation was initiated with adipocyte differentiation medium for 7 days and maintained in
162 adipocyte maintenance medium for additional 7 days. All media used for human primary
163 adipocyte culture were purchased from Zen-bio. The cells were used 14 days post initiation of
164 the differentiation.

165

166 *NOD1 ligand stimulation*

167 Differentiated 3T3-L1 adipocytes (at D9) were serum starved in DMEM containing
168 0.25% FBS for 12-15hr and stimulated with vehicle control, Tri-DAP, iE-DAP as indicated.

Total RNA and media were collected for chemokine/cytokine mRNA expression and protein secretion analysis. For insulin-stimulated Akt experiments, cells were pretreated with Tri-DAP as indicated and then stimulated with insulin (20nM) for 20min. For IRS-1 experiments, the cells were then stimulated with insulin for 5min. The cells were lysed with 1xRIPA buffer (Cell signaling) for 15min on ice and followed by vortex and sonication for 5 seconds. Total cell lysates were prepared after centrifugation at 4^0C for 15min to remove the insoluble materials and fat layer and were subjected to western blot analysis.

RNA preparation and quantitative real time PCR analysis

At indicated times, total RNA was prepared from adipocytes using Trizol (Invitrogen Corporation, Carlsbad, CA) according to the manufacturer's instruction. Total RNA abundance was quantified using a NanoDrop ND-1000 Spectrophotometer (NanoDrop Technologies, Wilmington, DE). Reverse transcription was carried out using High Capacity reverse transcription kit (Applied Biosystems, Foster City, CA) according the manufacturer's instruction. mRNA expression of NOD1, NOD2, TLR4, TLR2, various chemokines/cytokines, and loading control genes (18S and 36B4) were measured quantitatively using gene-specific TaqMan gene expression assays (Applied Biosystems) and were run in a 96-well format using an ABI 7300HT instrument. Cycle conditions were 50 ^{0}C 2min, 95 ^{0}C 15 min, then 40 cycles of 95 ^{0}C for 15 s/60 ^{0}C for 1 min.

Western blot analysis

The protein concentration was determined by BCA assay kit (Thermo Scientific, Waltham, MA). Thirty micrograms of total cell lysates were subjected to 10% SDS-PAGE and

transferred to polyvinylidene difluoride membrane (Bio-Rad, Hercules, CA). The membrane was blocked in 20 mM Tris–HCl, 137 mM NaCl, and 0.1% (v/v) Tween 20 (pH 7.4) containing 5% non-fat milk. The membrane was immunoblotted with primary antibodies for 1–24 hr, followed by secondary antibody coupled to horseradish peroxidase (GE Healthcare, Piscataway, NJ) for 1 hr. The membrane was exposed on an X-ray film using ECL Western blot detection reagents (GE Healthcare). To reprobe with different antibodies, the membrane was stripped in stripping buffer containing 62.5 mM Tris–HCl, 2% SDS and 100 mM 2-mercaptoethanol at 50 ^{0}C for 20-30 min. The signal was quantified by densitometry using ChemiDocXRS+ imaging system with image lab software (Bio-Rad).

Measurement of chemokine/cytokine

The supernatant from 3T3-L1 and human primary adipocyte cultures that were stimulated with different stimulus were collected and the level of MCP-1, RANTES, IL-6 and IL-8 were determined by enzyme-linked immunosorbent assay (ELISA) using Quantikine kits (R&D Systems Inc., Minneapolis, MN).

Small RNA interference

Small RNA interference against NOD1, NOD2, TLR4 and TLR2 were performed in differentiated 3T3-L1 adipocytes. SiRNA oligo targeting against murine NOD1, NOD2, TLR4 and TLR2 were from *Silencer Select* from Ambion and were transfected into 3T3-L1 adipocytes with DeliverX plus system (Panomics) according to the manufacturer's protocol.

Glucose uptake assay

Insulin-stimulated glucose uptake in 3T3-L1 adipocytes was determined by measuring [^{3}H] deoxy glucose uptake as described (14). Briefly, differentiated 3T3-L1 adipocytes (D9) were washed twice with PBS and incubated in serum free, low-glucose DMEM for 2-3 hr at 37 ^{0}C. The cells were washed once and incubated with Krebs-Ringer Phosphate buffer containing 0.25% BSA for 3 or 24 hr in the presence or absence of NOD1 ligand Tri-DAP (10 μg/ml). The cells were pretreated with cytochalasin B (a cell-permeable mycotoxin that blocks the translocation of glucose transporters) or vehicle control, followed by stimulation with or without insulin (20 nM) for 15min. Glucose uptake were initiated by the addition of [^{3}H] deoxy glucose (PerkinElmer, Waltham, MA) into the adipocyte culture for 5 min. The reaction was terminated by merging the dished in ice-cold PBS and washing with ice-cold PBS for 4 times. The cells were extracted by 0.05% SDS in 1xPBS and subjected to scintillation counting for [^{3}H] radioactivity. The specific insulin-induced glucose uptakes were calculated by subtracting the radioactivities of cytochalasin B treated samples from those of the vehicle treated samples. The radioactivity of each sample was normalized by the protein concentration. The data were expressed as cpm/μg of protein. For siRNA experiments, differentiated 3T3-L1 adipocytes were transfected with siRNA oligo targeting against NOD1 or non-targeting controls on day 1 and day 3 and the glucose uptake assays were performed after 72hr siRNA transfection.

Statistical Analysis

All data were presented as means ± SE. Each experiment was repeated at least 3 times. Within an experiment, measurements were performed in triplicates. Data were Log transformed when appropriate. Statistical analysis was performed using SigmaPlot 11.0 (Systat Software, Inc.). One way ANOVA with repeated measures followed by multiple comparisons test (Student-

Newman-Keuls Method) were performed to determine the differences between the treatment groups and/or time points. Student's t-test was performed when appropriate. The level of significance was set at $P < 0.05$.

Results

NOD1 and NOD2 mRNA are markedly increased during differentiation of 3T3-L1 and human primary culture derived from the subcutaneous fat.

TLR4 (32, 37) and TLR2 (32) mRNA level in pre- and adipocyte state have been studied in 3T3-L1 cells and their functionalities have been demonstrated in 3T3-L1 (25, 31, 32) and human primary adipocytes (24). Although NOD1 and NOD2 mRNA expression in 3T3-L1 preadipocytes and human primary peadipocytes have been reported (38), their expression in adipocyte state have not been studied. Therefore, we examined the changes of mRNA expression of NOD1 and NOD2 upon differentiation in 3T3-L1 cells and compared their mRNA expression to that of TLR4 and TLR2 in preadipocyte and adipocyte state.. The levels of gene expression are relative to 36B4, a gene that was reported not changed upon 3T3-L1 differentiation (41). Upon differentiation, NOD1 mRNA level was markedly increased and reached the highest peak at ~6 fold at D5, compared to D0. It reached to ~4 fold of that of RAW264.7 cells (a murine monocytic/macrophage cell line) at D8 (Fig. 1A). NOD2 mRNA level was also remarkably increased upon differentiation. It reached the highest peak of ~40 fold at D5, compared to D0 (Fig. 1A). The relative mRNA expression profiles of NOD1, NOD2, TLR4 and TLR2 change with differentiation state. The relative NOD1 mRNA expression was ~68 and ~10 fold of NOD2 in pre-and adipocyte state, respectively (Fig. 1B). TLR4 and TLR2 mRNA were expressed in both pre- and adipocytes, consistent with other reports (31, 32, 37). TLR4 and TLR2 mRNA

level was 2 and 6 fold of NOD1, respectively, in preadipocytes, and was ~2 and less than 1 fold of NOD1 in adipocytes (Fig. 1B). Moreover, we examined NOD1, NOD2 expression in pre-, adipocyte state and during adipocyte conversion of human primary preadipocyte culture derived from the subcutaneous fat. NOD1 mRNA was increased by 85% at D14; NOD2 mRNA was barely detectable in preadipocytes, and was increased by 338% at D14, compared to D0 ($p<0.05$) (Fig. 1C). Similar up-regulation of TLR4 and TLR2 mRNA level were observed during human adipocyte conversion ($p<0.01$) (Fig. 1C).

NOD1 mRNA is markedly increased in the fat tissues in diet-induced obese mice, but not in genetically obese ob/ob mice.

To probe the role of NOD1 and NOD2 in vivo, we studied their mRNA expression in diet-induced obese (DIO) and genetically obese mice models. NOD1 mRNA was increased to 2.5 fold ($p<0.01$) and 2.2 fold ($p<0.05$) of the chow-fed controls in the epididymal and subcutaneous fat tissues, respectively, of the DIO mice (Fig. 2A). NOD2 mRNA level was slightly increased in the epididymal fat of DIO mice (Fig. 2A), but was undetectable in the subcutaneous fat of the chow-fed controls and barely detectable in the DIO mice (data not shown). Both TLR4 and TLR2 mRNA were significantly increased in the fat tissues of the DIO mice ($p<0.05$). In contrast, NOD1 mRNA was not increased in leptin deficient *ob/ob* mice in both fat tissues, compared to the controls (Fig. 2B). On the other hand, NOD2, TLR4 and TLR2 mRNA were significantly increased in both fat tissues of the *ob/ob* mice ($p<0.05$ and $p<0.01$) (Fig. 2B). In 3T3-L1 preadipocytes, NOD1, but not NOD2 activation, by its synthetic ligand was shown to induce proinflammatory cytokine expression (38). Because of the higher mRNA level

283 of NOD1 in adipocytes and in fat tissues of the DIO mice and that the role of NOD1 in
284 adipocytes has not been studied, we chose to focus on NOD1 in adipocytes in this study.

285

286 ***NOD1 activation induces proinflammatory chemokine and cytokine expression in adipocytes.***

287 We examined whether activation of NOD1 by the synthetic ligands can induce
288 proinflammatory chemokine/cytokine response in 3T3-L1 adipocytes. To confirm the stimulating
289 specificity of Tri-DAP and iE-DAP preparation used, we tested them in 293T reconstituted
290 systems as described previously (49). Consistent with being reported (4, 12), the preparation of
291 Tri-DAP and iE-DAP stimulated NF-κB activation in 293T transfected with NOD1 expression
292 plasmid, but not with TLR4 or TLR2 expression plasmid (data not shown), demonstrating the
293 specificity of NOD1 activation by Tri-DAP or iE-DAP in our experiments.

294 We focused on proinflammatory MCP-1, TNF-α, IL-6, which are implicated in insulin
295 resistance (10, 33), as well as RANTES and MIP-2 (human IL-8 homolog), known target genes
296 of NOD1 activation (2). Tri-DAP dose-dependently induced MCP-1, RANTES, TNF-α and
297 MIP-2 mRNA expression ($p<0.05$) (Fig. 3A). The dose-dependent changes in MCP-1 and
298 RANTES protein secretion were confirmed by ELISA ($p<0.05$) (Fig. 3B). The protein secretion
299 of TNF-α, MIP-2 and IL-6, however, were under detection limits (data not shown). Moreover,
300 Tri-DAP also dose-dependently induced proinflammatory MCP-1, IL-6 and IL-8 protein
301 secretion in human primary adipocytes differentiated from preadipocytes culture derived from
302 the subcutaneous fat ($p<0.05$) (Fig. 4A). Similar protein secretion patterns were observed when
303 another NOD1 synthetic ligand, iE-DAP, was used ($p<0.05$) (Fig. 4B). We chose the dose of
304 10μg/ml, the lower dose with significant effects, in further studies. Tri-DAP (10 μg/ml), not

vehicle control, induced MCP-1, RANTES, TNF-α and MIP2 in a time-dependent manner ($p<0.001$) (Fig. 5A). The time-dependent changes of MCP-1 and RANTES protein secretion by Tri-DAP were also confirmed by ELISA ($p<0.001$) (Fig. 5B). Furthermore, Tri-DAP (10μg/ml) time-dependently induced MCP-1, RANTES, IL-6, IL-8 and TNF-α mRNA expression ($p<0.001$) (Fig. 6A) and MCP-1, IL-6 and IL-8 protein secretion ($p<0.001$) (Fig. 6B) in human primary adipocytes. RANTES and TNF-α protein secretion in human primary adipocytes were under detection limits (data not shown).

NOD1 activation induces activation of NF-κB and MAPK signaling pathways, leading to proinflammatory gene expression, in adipocytes.

It has been shown that NOD1 activation induces activation of NF-κB and MAPK signaling pathways, leading to proinflammatory responses in many cell types (8, 16). Therefore, we determined whether NOD1 activation by Tri-DAP in 3T3-L1 adipocytes induced activation of these signaling events. NOD1 activation by Tri-DAP induced NF-κB activation as revealed by phosphorylation of NF-κB p65 and IκBα (Fig.7A) and activation of NF-κB reporter gene (Fig.7B). NOD1 activation also induced phosphorylation of p38, JNK and ERK1/2 in adipocytes (Fig.7D). To determine whether activation of these signaling pathways is required for the proinflammatory gene expression induced by Tri-DAP, we employed pharmacological inhibitors. NF-κB inhibitor Caffeic acid phenethyl ester (CAPE) and Bay117821 (Bay) significantly inhibited Tri-DAP-induced MCP-1 and RANTES mRNA ($p<0.01$) (Fig. 7C). Similarly, pharmacological inhibitor of p38 (SB203580), JNK (SP600125) or ERK (PD98054) also significantly inhibited Tri-DAP-induced MCP-1 ($p<0.01$ and $p<0.05$). In contrast,

pharmacological inhibitor of p38 and JNK, but not inhibitor of ERK, significantly inhibited Tri-DAP-induced RANTES mRNA ($p<0.01$) (Fig.7E). Together, these results demonstrate that Tri-DAP induces proinflammatory gene expression via activation of NF-κB and MAPK signaling pathways in adipocytes and that proinflammatory MCP-1 and RANTES gene expression may be controlled by distinct intracellular signaling pathways downstream of NOD1 activation.

NOD1 activation suppresses insulin signaling and glucose uptake in 3T3-L1 adipocytes.

To further explore the role of NOD1 in adipose inflammation and insulin resistance, we sought to examine the effects of NOD1 activation on insulin signaling. Insulin-stimulated phosphorylation of Akt on Ser473 and Thr 308 residues, the commonly used markers of insulin signaling (21, 42, 45), were evaluated. Tri-DAP suppressed insulin-induced phosphorylation of Akt on Ser 473 and Thr308 at 24hr, with more suppression observed on Ser 473 than on Thr 308. Consistently, the phosphorylation of Akt downstream target GSK3α/3β was also suppressed at 24hr (Fig. 8A). No apparent suppression of insulin-induced phosphorylation of Akt and GSK3α/3β were observed by NOD1 stimulation at 3hr (Fig. 8A). We also examined upstream insulin signaling events. Tri-DAP decreased pan-tyrosine phosphorylation of Insulin receptor substrate 1 (IRS-1) at both 3hr and 24hr; decreased specific tyrosine phosphorylation of IRS-1 on Tyr 632 only at 24hr; and increased inhibitory serine phosphorylation of IRS-1 on Ser 612 at 3hr (Fig. 8B). No change on IRS-1 Ser 307 phosphorylation was observed (data not shown). Together, these results demonstrate that NOD1 activation impairs IRS-1 tyrosine phosphorylation, leading to impaired downstream phosphorylation of Akt and GSK.

To explore whether attenuated insulin signaling by NOD1 activation leads to insulin resistance, we evaluated insulin-induced glucose uptake by measuring insulin-stimulated [^{3}H] deoxy-glucose uptake into the 3T3-L1 adipocytes. Insulin treatment (20nM) induced around two fold glucose uptake in the control cells, but was suppressed by ~40% ($p<0.05$) after NOD1 stimulation for 24hr (Fig. 9B). 3hr-treatment of Tri-DAP did not significantly suppress insulin-induced glucose uptake (Fig. 9A). These data are consistent with the effects of Tri-DAP on insulin signaling shown in Fig.8.

Tri-DAP-induced proinflammatory response and decrease in insulin-induced glucose uptake in adipocytes were via NOD1.

To further confirm the observed effects of Tri-DAP in inducing proinflammatory gene expression and reducing insulin-induced glucose uptake in adipocytes is mediated through NOD1, we employed siRNA against NOD1, NOD2, TLR4 and TLR2 in adipocytes. As shown in Fig. 10A, all three siRNA targeting against NOD1, but not the other siRNA oligos, reduced NOD1 mRNA by 60-80% in 3T3-L1 adipocytes. All three siRNA targeting NOD1, but not the siRNA targeting TLR4, TLR2 or NOD2, significantly reduced Tri-DAP-induced MCP-1 by 50-65% ($p<0.01$) and RANTES mRNA by 62-78% ($p<0.01$) (Fig. 10B). MCP-1 and RANTES protein levels were consistent with the mRNA expression (Fig. 10C). Tri-DAP-induced TNF-α and MIP-2 mRNA were also reduced by siRNA targeting NOD1 ($p<0.01$), not by siRNA targeting TLR4, TLR2 and NOD2 (data not shown). Moreover, the siRNA targeting Nod1 decreased Tri-DAP-induced NF-κB activation by ~50% ($p<0.05$), as revealed by NF-κB reporter gene (Fig. 10C). Furthermore, the siRNA targeting NOD1 reversed Tri-DAP-induced

suppression of insulin-induced glucose uptake ($p<0.05$) (Fig. 10D). Together, these results demonstrate the specific role of NOD1 in observed proinflammatory response and insulin resistance induced by Tri-DAP in adipocytes.

Discussion

Chronic inflammation, as characterized by macrophage infiltration and proinflammatory cytokine/chemokine secretion, is associated with obesity and insulin resistance (43, 44, 47). However, the underlying mechanisms are not fully understood. Membrane-bound pattern recognition receptors, TLR4 and TLR2 in particular, have been suggested to be involved in developing adipose inflammation and insulin resistance (15, 30, 36, 39). Here we show, for the first time, the role of NOD1, a cytosolic PRR, in proinflammatory response and insulin resistance in adipocytes. NOD1 and NOD2 mRNA are markedly increased upon differentiation of murine 3T3-L1 adipocytes and human primary adipocytes; NOD1 mRNA is increased in the fat tissues of the DIO mice, but not in the *ob/ob* mice, compared with controls; activation of NOD1 by the synthetic ligand Tri-DAP induces MAPK and NF-κB-mediated proinflammatory gene expression and suppression of insulin signaling, and insulin-induced glucose uptake in adipocytes. To confirm the specificity of the role of NOD1, we show that Tri-DAP-induced MCP-1 and RANTES mRNA and protein expression are blocked by the siRNA targeting NOD1, but not by the siRNA targeting TLR4, TLR2 or NOD2. Moreover, Tri-DAP-induced NF-κB activation and suppression of insulin-induced glucose uptake are attenuated by the siRNA targeting NOD1. Together, our results suggest that NOD1 may play an important role in adipose inflammation and insulin resistance in diet-induced obesity.

NOD1 activation by Tri-DAP induces proinflammatory MCP-1, RANTES, TNF-α, IL-6 and IL-8 mRNA expression both in 3T3-L1 adipocytes as well as in human primary adipocyte culture (Fig. 3-6). MCP-1, a chemoattract factor for monocyte/ macrophage, is critical for macrophage infiltration into adipose tissue, which is thought to be the initial step leading to adipose inflammation (18, 19, 47). TNF-α and IL-6 are known cytokines that can induce insulin resistance. In addition, RANTES has been reported to be up-regulated and associated with T-cell accumulation in murine and human obesity (46), which contributs to adipose inflammation and metabolic syndrome. Recently, it has been reported that neutrophils transiently infiltrate intra-abdominal fat early under high fat feeding in mice (7). CXC chemokines including IL-8, MIP-2 are among the most critical inflammatory mediators for recruitment of neutrophils (23). Our results suggest that NOD1 activation may facilitate the infiltration of macrophages as well as T-cells and neutrophils into adipose tissue, leading to adipose inflammation. Moreover, NOD1-mediated secretions of proinflammatory cytokines from adipocytes may directly contribute to insulin resistance. Consistently, we show that NOD1 activation induces attenuation of insulin-signaling, which leads to suppression of insulin-induced glucose uptakes.

The mechanisms underlying the proinflammatory gene expression downstream of NOD1 activation in adipocytes seem to involve both NF-κB and MAPK signaling pathways. The fact that NF-κB pathway is essential for both MCP-1 and RANTES mRNA expression but ERK1/2 is only necessary for MCP-1, not RANTES, mRNA expression (Fig.7C and E) suggests that proinflammatory gene expression downstream of NOD1 activation is controlled by distinct intracellular pathways in adipocytes, consistent with NOD1 results in other systems (2).

How the signaling events downstream of NOD1 activation interact with insulin signaling, leading to insulin resistance in adipocytes remain to be determined. NOD1 activation induces activation of p38, JNK, and ERK1/2 MAPK as well as NF-κB pathway in 3T3-L1 adipocytes (Fig. 7). It has been reported that JNK, ERK1/2 and IKKβ (a component of IKK complex that activates NF-κB) can phosphorylate insulin receptor substrate 1(IRS-1) on serine residues (1, 5, 11), which in turn inhibits tyrosine phosphorylation of IRS-1, required for the activation of insulin signaling. It remains to be determined whether activation of JNK, ERK1/2 and p38 MAPK and IKKβ upon NOD1 activation directly attenuate insulin signaling, or NOD1-mediated production of proinflammatory cytokines/chemokines, e.g.,TNF-α, IL-6 and MCP-1, interfere with insulin signaling in auto- and/or paracrine fashion, leading to insulin resistance in adipocytes. TNF-α, IL-6 and MCP-1 are known to alter insulin signaling through activation of S6 protein kinase (S6K) (48), mammalian target of rapamycine (mTOR) (22) and ERK1/2 (34), respectively. Understanding the signaling events downstream of NOD1 activation as it interfaces with insulin signaling may provide novel targets for treating obesity-associated inflammation and insulin resistance.

Previously we have shown that NOD1 can be activated by SFA, leading to NF-κB activation and proinflammatory target gene expression in human intestinal epithelial HCT116 cells and 293T reconstituted with NOD1 expression plasmid (49). High free fatty acids (FFA) found in obese subjects are thought to be the metabolic signal to induce inflammation in obese state (3). But the primary molecular mechanisms by which FFAs cause inflammation and insulin

resistance are not fully understood and the roles of TLRs, TLR4 and TLR2 in particular, in diet-induced obesity, adipose inflammation and insulin resistance have been suggested (15, 36). In light of our early studies and the results that NOD1 is expressed and functional in adipocytes, it warrants further investigation whether NOD1 plays an important role in SFA- and/or high fat diet-induced obesity, inflammation and insulin resistance. Consistently, NOD1 mRNA is found to be increased in the fat tissues of the DIO mice, but not in genetically obese *ob/ob* mice, while TLR4 and TLR2 mRNA are induced in both obesity models (Fig. 2), suggesting a unique role for NOD1 in diet-induced obesity. Although the relative mRNA level of NOD1 is lower than or similar to that of TLR4 or TLR2 in 3T3-L1 pre- and adipocytes (Fig. 1B), further studies are warranted to dissect the relative contributions of each PRR to adipose inflammation and insulin resistance in diet-induced obesity.

In conclusion, we show that NOD1 activation induces MAPK and NF-κB-mediated proinflammatory gene expression and suppresses insulin signaling and subsequent glucose uptake in adipocytes. Our results lay the ground work for future studies on the role of NOD1 in diet-induced obesity, inflammation and insulin resistance. Understanding the role of NOD1 in obesity-associated inflammation and insulin resistance may provide novel strategies to prevent and/or treat obesity and insulin resistance.

Acknowledgement

The work was supported by faculty start-up funds from The University of Tennessee to L.Z. Dr. Yijun Zhou current address is Department of Endocrinology and Metabolism, The fourth Affiliated Hospital of China Medical University, Shenyang, China.

Figure Legend

Fig. 1 NOD1, NOD2, TLR4 and TLR2 mRNA expression during adipocyte differentiation. (A, B) 3T3-L1 preadipocytes were grown into confluency and then were differentiated into adipocytes as described under materials and methods. Total RNA was isolated 2 day before confluency (D-2), at confluency (D0), 3-(D3), 4-(D4), 5-(D5) and 8-day (D8) post initiation of differentiation. mRNA expression of various receptors were evaluated by quantitative RT-PCR using TaqMan expression assays. (A) Time course of NOD1 and NOD2 mRNA expression during 3T3-L1 adipocyte differentiation. The relative mRNA expression was normalized to 34B4 and expressed as fold of D0 value (set as 1). (B) Relative mRNA expression of TLR4, TLR2, NOD1 and NOD2 in 3T3-L1 preadipocyte (D0) and adipocyte state (D8). The relative mRNA expression was normalized to 36B4 and expressed as fold of NOD2 value (set as 1). (C) Primary human preadipocytes derived from the subcutaneous fat were differentiated into adipocytes. mRNA expression of NOD1, NOD2, TLR4 and TLR2 were evaluated by quantitative RT-PCR. The relative expression was normalized to 18S and expressed as fold of D0 value (set as 1). Data are mean±SE (n=3). *,**, significantly different from the controls with $p<0.05$ and $p<0.01$, respectively. RAW, RAW264.7 macrophages.

Fig. 2 NOD1 and NOD2 mRNA expression in the fat tissues from the DIO and ob/ob mice. NOD1, NOD2, TLR4 and TLR2 mRNA expression were evaluated by quantitative RT-PCR using TaqMan expression assays in the epididymal and subcutaneous fat pads from the DIO male mice (n=7) (A) and *ob/ob* male mice (n=6) (B). *, **, significantly different from the controls with $p<0.05$ and $p<0.01$, respectively.

Fig. 3 NOD1 ligand Tri-DAP induced proinflammatory chemokine and cytokine expression in 3T3-L1 adipocytes in a dose-dependent manner. 3T3-L1 adipocytes were stimulated with increasing doses of Tri-DAP (0, 1, 10, 50μg/ml) for 15hr. (A) Relative mRNA expression of MCP-1, RANTES, TNF-α, MIP-2 and IL-6 were evaluated by quantitative RT-PCR. The relative gene expression was normalized to 18S. Data are expressed as fold of vehicle value (set as 1). (B) MCP-1 and RANTES protein secretion in the supernatant of adipocytes stimulated with Tri-DAP were evaluated by ELISA. Data are mean±SE (n=3). NS, not significant.

Fig. 4 NOD1 ligands induced proinflammatory chemokine and cytokine expression in human primary adipocytes differentiated from preadipocytes derived from the subcutaneous fat in a dose-dependent manner. Human primary adipocytes were stimulated with increasing doses of Tri-DAP (0, 10, 50μg/ml) (A) or iE-DAP (0, 10, 100μg/ml) (B) for 15hr. MCP-1, IL-6 and IL-8 protein secretion in the supernatant of adipocytes stimulated with Tri-DAP or iE-DAP were evaluated by ELISA. Data are mean±SE (n=3).

Fig. 5 NOD1 ligand Tri-DAP induced proinflammatory chemokine and cytokine expression in 3T3-L1 adipocytes in a time dependent manner. 3T3-L1 adipocytes were stimulated with vehicle (open circle) or Tri-DAP (10μg/ml, closed circle) for 0, 4, 8, 12, 24, and 48hr. (A) Relative mRNA expression of MCP-1, RANTES, TNF-α, MIP-2 and IL-6 were evaluated by quantitative PCR. The relative gene expression was normalized to 18S. Data are expressed as fold of time 0 value (set as 1). (B) MCP-1 and RANTES protein secretion in the supernatant of adipocytes stimulated with Tri-DAP were evaluated by ELISA. Data are mean±SE (n=3). NS, not significant.

Fig. 6 NOD1 ligand Tri-DAP induced proinflammatory chemokine and cytokine expression in human primary adipocytes differentiated from preadipocytes derived from the subcutaneous fat in a time dependent manner. Human primary adipocytes were stimulated with vehicle (open circle) or Tri-DAP (10μg/ml, closed circle) for 0, 4, 8, 12, 24, and 48hr. (A) Relative mRNA expression of MCP-1, RANTES, IL-6, IL-8 and TNF-α were evaluated by quantitative PCR. The relative gene expression was normalized to 18S. Data are expressed as fold of time 0 value (set as 1). (B) MCP-1, IL-6 and IL-8 protein secretion in the supernatant of adipocytes stimulated with Tri-DAP were evaluated by ELISA. Data are mean±SE (n=3). NS, not significant.

Fig. 7 NOD1 ligand Tri-DAP induced activation of NF-κB and MAPK signaling pathways. 3T3-L1 adipocytes were stimulated with vehicle or Tri-DAP (10μg/ml) for indicated periods of time and whole cell lysate were prepared and analyzed with specific antibodies against phospho-

p65, p65, phospho-IκBα and loading control tubulin (A), phospho-p38, phospho-JNK, phospho-ERK, p38, JNK and ERK (C). The intensity of bands were quantified by densitometry and expressed as ratio of phosphorylated protein to the total protein. The ratio was normalized to the control (set at 1). (B) 3T3-L1 adipocytes were infected with adenovirus coding for NF-κB-luciferase and β-galactosidase reporter for 24hr and the cells were stimulated with increasing doses of Tri-DAP for 10hr. Reporter gene assays were performed. Relative luciferase activity was normalized with β-galactosidase activity. (C, E) 3T3-L1 adipocytes were pretreated with vehicle control or NF-κB inhibitor Caffeic acid phenethyl ester (CAPE) or Bay117821 (Bay) (C) or pharmacological inhibitor of p38 (SB203580), JNK (SP600125) or ERK (PD98054) (E) for 1hr before stimulated with Tri-DAP for 12hr. Relative gene expression of MCP-1 and RANTES were analyzed. *, **, significantly different from the controls with $p<0.05$ and $p<0.01$, respectively.

Fig. 8 NOD1 ligand Tri-DAP suppressed insulin signaling. (A) 3T3-L1 adipocytes were stimulated with Tri-DAP (10 μg/ml) or vehicle for 3 and 24hr followed by insulin stimulation for 20 min. The whole cell lysate were prepared. The phosphorylation of Akt on Ser 473 and Thr 308, Akt, phosphorylation of GSK3α/3β on Ser 21/9 and loading control β-actin were analyzed. (B) 3T3-L1 adipocytes were stimulated with Tri-DAP (10, 50 μg/ml) or vehicle for 3 and 24hr followed by insulin stimulation for 5 min. The whole cell lysate were prepared. The phosphorylation of IRS-1, IRS-1 and loading control tubulin were analyzed. The intensity of bands were quantified by densitometry and expressed as ratio of phosphorylated protein to the total protein. The ratio was normalized to the control (set as 1).

Fig. 9 NOD1 ligand Tri-DAP suppressed insulin-induced glucose uptake in 3T3-L1 adipocytes. 3T3-L1 adipocytes were starved in Krebs-Ringer Phosphate buffer containing 0.25% BSA in the presence of Tri-DAP (10μg/ml) for 3 or 24hr, followed by insulin-induced glucose uptake assay as described under materials and methods. The radioactivity of each sample was normalized by protein concentration. Data are mean±SE (n=3) and expressed as CPM/μg. *, significantly different from the controls with $p<0.05$.

Fig. 10 Tri-DAP-induced proinflammatory response and decreased in insulin-induced glucose uptake in adipocytes were via NOD1. (A) 3T3-L1 adipocytes were transfected with siRNA targeting against NOD1, NOD2, TLR4, TLR2 or non-targeting control. NOD1 mRNA was evaluated by quantitative RT-PCR using TaqMan expression assays. (B, C) 3T3-L1 adipocytes were transfected with siRNA targeting against NOD1, NOD2, TLR4, TLR2 or non-targeting control for 24hr followed by stimulation of Tri-DAP for additional 24hr. Relative gene expression of MCP-1 and RANTES were analyzed (B). The relative gene expression was normalized to 18S. Data are expressed as fold of vehicle treated non-targeting cells (set as 1). MCP-1 and RANTES protein levels from the supernatant of cells in (B) were evaluated by ELISA (C). (D) 3T3-L1 adipocytes were transfected with siRNA targeting against NOD1 or non-targeting control for 24hr, followed by infection with NF-κB luciferase reporter and β-galactosidase containing adenovirus for 15hr. The cells were then stimulated with Tri-DAP. Reporter gene assays were performed. Relative luciferase activity was normalized with β-galactosidase activity. (E) 3T3-L1 adipocytes were transfected with siRNA targeting against

NOD1 or non-targeting control. The cells were then stimulated with Tri-DAP for 24hr. Insulin-induced glucose uptake assays were performed. Insulin-induced glucose uptake in non-targeting siRNA oligo-transfected cells was set at 100%. Data are mean±SE (n=3). *, **, significantly different from the controls with $p<0.05$ and $p<0.01$, respectively.

Reference

1. **Aguirre V, Uchida T, Yenush L, Davis R, and White MF**. The c-Jun NH(2)-terminal kinase promotes insulin resistance during association with insulin receptor substrate-1 and phosphorylation of Ser(307). *J Biol Chem* 275: 9047-9054, 2000.
2. **Berube J, Bourdon C, Yao Y, and Rousseau S**. Distinct intracellular signaling pathways control the synthesis of IL-8 and RANTES in TLR1/TLR2, TLR3 or NOD1 activated human airway epithelial cells. *Cell Signal* 21: 448-456, 2009.
3. **Boden G**. Obesity and free fatty acids. *Endocrinol Metab Clin North Am* 37: 635-646, viii-ix, 2008.
4. **Chamaillard M, Hashimoto M, Horie Y, Masumoto J, Qiu S, Saab L, Ogura Y, Kawasaki A, Fukase K, Kusumoto S, Valvano MA, Foster SJ, Mak TW, Nunez G, and Inohara N**. An essential role for NOD1 in host recognition of bacterial peptidoglycan containing diaminopimelic acid. *Nat Immunol* 4: 702-707, 2003.
5. **De Fea K, and Roth RA**. Modulation of insulin receptor substrate-1 tyrosine phosphorylation and function by mitogen-activated protein kinase. *The Journal of biological chemistry* 272: 31400-31406, 1997.
6. **Ehses JA, Meier DT, Wueest S, Rytka J, Boller S, Wielinga PY, Schraenen A, Lemaire K, Debray S, Van Lommel L, Pospisilik JA, Tschopp O, Schultze SM, Malipiero U, Esterbauer H, Ellingsgaard H, Rutti S, Schuit FC, Lutz TA, Boni-Schnetzler M, Konrad D, and Donath MY**. Toll-like receptor 2-deficient mice are protected from insulin resistance and beta cell dysfunction induced by a high-fat diet. *Diabetologia* 53: 1795-1806, 2010.
7. **Elgazar-Carmon V, Rudich A, Hadad N, and Levy R**. Neutrophils transiently infiltrate intra-abdominal fat early in the course of high-fat feeding. *J Lipid Res* 49: 1894-1903, 2008.
8. **Franchi L, Warner N, Viani K, and Nunez G**. Function of Nod-like receptors in microbial recognition and host defense. *Immunol Rev* 227: 106-128, 2009.
9. **Fritz JH, Ferrero RL, Philpott DJ, and Girardin SE**. Nod-like proteins in immunity, inflammation and disease. *Nat Immunol* 7: 1250-1257, 2006.
10. **Galic S, Oakhill JS, and Steinberg GR**. Adipose tissue as an endocrine organ. *Mol Cell Endocrinol* 316: 129-139, 2010.
11. **Gao Z, Hwang D, Bataille F, Lefevre M, York D, Quon MJ, and Ye J**. Serine phosphorylation of insulin receptor substrate 1 by inhibitor kappa B kinase complex. *J Biol Chem* 277: 48115-48121, 2002.
12. **Girardin SE, Boneca IG, Carneiro LA, Antignac A, Jehanno M, Viala J, Tedin K, Taha MK, Labigne A, Zahringer U, Coyle AJ, DiStefano PS, Bertin J, Sansonetti PJ, and Philpott DJ**. Nod1 detects a unique muropeptide from gram-negative bacterial peptidoglycan. *Science* 300: 1584-1587, 2003.
13. **Girardin SE, Boneca IG, Viala J, Chamaillard M, Labigne A, Thomas G, Philpott DJ, and Sansonetti PJ**. Nod2 is a general sensor of peptidoglycan through muramyl dipeptide (MDP) detection. *J Biol Chem* 278: 8869-8872, 2003.
14. **Hausdorff SF, Fingar DC, Morioka K, Garza LA, Whiteman EL, Summers SA, and Birnbaum MJ**. Identification of wortmannin-sensitive targets in 3T3-L1 adipocytes. DissociationoOf insulin-stimulated glucose uptake and glut4 translocation. *J Biol Chem* 274: 24677-24684, 1999.
15. **Himes RW, and Smith CW**. Tlr2 is critical for diet-induced metabolic syndrome in a murine model. *FASEB J* 2009.
16. **Inohara, Chamaillard, McDonald C, and Nunez G**. NOD-LRR proteins: role in host-microbial interactions and inflammatory disease. *Annu Rev Biochem* 74: 355-383, 2005.
17. **Inohara N, Ogura Y, Fontalba A, Gutierrez O, Pons F, Crespo J, Fukase K, Inamura S, Kusumoto S, Hashimoto M, Foster SJ, Moran AP, Fernandez-Luna JL, and Nunez G**. Host recognition of bacterial

615 muramyl dipeptide mediated through NOD2. Implications for Crohn's disease. *J Biol Chem* 278: 5509-
616 5512, 2003.
617 18. **Kamei N, Tobe K, Suzuki R, Ohsugi M, Watanabe T, Kubota N, Ohtsuka-Kowatari N, Kumagai K,**
618 **Sakamoto K, Kobayashi M, Yamauchi T, Ueki K, Oishi Y, Nishimura S, Manabe I, Hashimoto H, Ohnishi**
619 **Y, Ogata H, Tokuyama K, Tsunoda M, Ide T, Murakami K, Nagai R, and Kadowaki T**. Overexpression of
620 monocyte chemoattractant protein-1 in adipose tissues causes macrophage recruitment and insulin
621 resistance. *J Biol Chem* 281: 26602-26614, 2006.
622 19. **Kanda H, Tateya S, Tamori Y, Kotani K, Hiasa K, Kitazawa R, Kitazawa S, Miyachi H, Maeda S,**
623 **Egashira K, and Kasuga M**. MCP-1 contributes to macrophage infiltration into adipose tissue, insulin
624 resistance, and hepatic steatosis in obesity. *J Clin Invest* 116: 1494-1505, 2006.
625 20. **Kawai T, and Akira S**. The role of pattern-recognition receptors in innate immunity: update on
626 Toll-like receptors. *Nat Immunol* 11: 373-384, 2010.
627 21. **Kienesberger PC, Lee D, Pulinilkunnil T, Brenner DS, Cai L, Magnes C, Koefeler HC, Streith IE,**
628 **Rechberger GN, Haemmerle G, Flier JS, Zechner R, Kim YB, and Kershaw EE**. Adipose triglyceride lipase
629 deficiency causes tissue-specific changes in insulin signaling. *J Biol Chem* 284: 30218-30229, 2009.
630 22. **Kim JH, Kim JE, Liu HY, Cao W, and Chen J**. Regulation of interleukin-6-induced hepatic insulin
631 resistance by mammalian target of rapamycin through the STAT3-SOCS3 pathway. *The Journal of*
632 *biological chemistry* 283: 708-715, 2008.
633 23. **Kobayashi Y**. The role of chemokines in neutrophil biology. *Front Biosci* 13: 2400-2407, 2008.
634 24. **Kopp A, Buechler C, Bala M, Neumeier M, Scholmerich J, and Schaffler A**. Toll-like receptor
635 ligands cause proinflammatory and prodiabetic activation of adipocytes via phosphorylation of
636 extracellular signal-regulated kinase and c-Jun N-terminal kinase but not interferon regulatory factor-3.
637 *Endocrinology* 151: 1097-1108, 2010.
638 25. **Kopp A, Buechler C, Neumeier M, Weigert J, Aslanidis C, Scholmerich J, and Schaffler A**. Innate
639 immunity and adipocyte function: ligand-specific activation of multiple Toll-like receptors modulates
640 cytokine, adipokine, and chemokine secretion in adipocytes. *Obesity (Silver Spring)* 17: 648-656, 2009.
641 26. **Lee JY, Sohn KH, Rhee SH, and Hwang D**. Saturated fatty acids, but not unsaturated fatty acids,
642 induce the expression of cyclooxygenase-2 mediated through Toll-like receptor 4. *J Biol Chem* 276:
643 16683-16689, 2001.
644 27. **Lee JY, Zhao L, and Hwang DH**. Modulation of pattern recognition receptor-mediated
645 inflammation and risk of chronic diseases by dietary fatty acids. *Nutr Rev* 68: 38-61, 2010.
646 28. **Lee JY, Zhao L, Youn HS, Weatherill AR, Tapping R, Feng L, Lee WH, Fitzgerald KA, and Hwang**
647 **DH**. Saturated fatty acid activates but polyunsaturated fatty acid inhibits Toll-like receptor 2 dimerized
648 with Toll-like receptor 6 or 1. *J Biol Chem* 279: 16971-16979, 2004.
649 29. **Oort PJ, Warden CH, Baumann TK, Knotts TA, and Adams SH**. Characterization of Tusc5, an
650 adipocyte gene co-expressed in peripheral neurons. *Mol Cell Endocrinol* 276: 24-35, 2007.
651 30. **Poggi M, Bastelica D, Gual P, Iglesias MA, Gremeaux T, Knauf C, Peiretti F, Verdier M, Juhan-**
652 **Vague I, Tanti JF, Burcelin R, and Alessi MC**. C3H/HeJ mice carrying a toll-like receptor 4 mutation are
653 protected against the development of insulin resistance in white adipose tissue in response to a high-fat
654 diet. *Diabetologia* 50: 1267-1276, 2007.
655 31. **Poulain-Godefroy O, and Froguel P**. Preadipocyte response and impairment of differentiation in
656 an inflammatory environment. *Biochem Biophys Res Commun* 356: 662-667, 2007.
657 32. **Poulain-Godefroy O, Le Bacquer O, Plancq P, Lecoeur C, Pattou F, Fruhbeck G, and Froguel P**.
658 Inflammatory role of Toll-like receptors in human and murine adipose tissue. *Mediators Inflamm* 2010:
659 823486, 2010.
660 33. **Rasouli N, and Kern PA**. Adipocytokines and the metabolic complications of obesity. *J Clin*
661 *Endocrinol Metab* 93: S64-73, 2008.

34. **Sell H, Dietze-Schroeder D, Kaiser U, and Eckel J**. Monocyte chemotactic protein-1 is a potential player in the negative cross-talk between adipose tissue and skeletal muscle. *Endocrinology* 147: 2458-2467, 2006.
35. **Senn JJ**. Toll-like receptor-2 is essential for the development of palmitate-induced insulin resistance in myotubes. *J Biol Chem* 281: 26865-26875, 2006.
36. **Shi H, Kokoeva MV, Inouye K, Tzameli I, Yin H, and Flier JS**. TLR4 links innate immunity and fatty acid-induced insulin resistance. *J Clin Invest* 116: 3015-3025, 2006.
37. **Song MJ, Kim KH, Yoon JM, and Kim JB**. Activation of Toll-like receptor 4 is associated with insulin resistance in adipocytes. *Biochem Biophys Res Commun* 346: 739-745, 2006.
38. **Stroh T, Batra A, Glauben R, Fedke I, Erben U, Kroesen A, Heimesaat MM, Bereswill S, Girardin S, Zeitz M, and Siegmund B**. Nucleotide oligomerization domains 1 and 2: regulation of expression and function in preadipocytes. *J Immunol* 181: 3620-3627, 2008.
39. **Suganami T, Mieda T, Itoh M, Shimoda Y, Kamei Y, and Ogawa Y**. Attenuation of obesity-induced adipose tissue inflammation in C3H/HeJ mice carrying a Toll-like receptor 4 mutation. *Biochem Biophys Res Commun* 354: 45-49, 2007.
40. **Takeuchi O, and Akira S**. Pattern recognition receptors and inflammation. *Cell* 140: 805-820, 2010.
41. **Thompson GM, Trainor D, Biswas C, LaCerte C, Berger JP, and Kelly LJ**. A high-capacity assay for PPARgamma ligand regulation of endogenous aP2 expression in 3T3-L1 cells. *Anal Biochem* 330: 21-28, 2004.
42. **Wada T, Hori S, Sugiyama M, Fujisawa E, Nakano T, Tsuneki H, Nagira K, Saito S, and Sasaoka T**. Progesterone inhibits glucose uptake by affecting diverse steps of insulin signaling in 3T3-L1 adipocytes. *Am J Physiol Endocrinol Metab* 2010.
43. **Weisberg SP, McCann D, Desai M, Rosenbaum M, Leibel RL, and Ferrante AW, Jr.** Obesity is associated with macrophage accumulation in adipose tissue. *J Clin Invest* 112: 1796-1808, 2003.
44. **Wellen KE, and Hotamisligil GS**. Obesity-induced inflammatory changes in adipose tissue. *J Clin Invest* 112: 1785-1788, 2003.
45. **Whelan SA, Dias WB, Lakshmanan T, Lane MD, and Hart GW**. Regulation of Insulin Receptor 1 (IRS-1)/AKT Kinase Mediated Insulin Signaling by O-linked {beta}-N-acetylglucosamine (O-GlcNAc) in 3T3-L1 Adipocytes. *J Biol Chem* 2009.
46. **Wu H, Ghosh S, Perrard XD, Feng L, Garcia GE, Perrard JL, Sweeney JF, Peterson LE, Chan L, Smith CW, and Ballantyne CM**. T-cell accumulation and regulated on activation, normal T cell expressed and secreted upregulation in adipose tissue in obesity. *Circulation* 115: 1029-1038, 2007.
47. **Xu H, Barnes GT, Yang Q, Tan G, Yang D, Chou CJ, Sole J, Nichols A, Ross JS, Tartaglia LA, and Chen H**. Chronic inflammation in fat plays a crucial role in the development of obesity-related insulin resistance. *J Clin Invest* 112: 1821-1830, 2003.
48. **Zhang J, Gao Z, Yin J, Quon MJ, and Ye J**. S6K directly phosphorylates IRS-1 on Ser-270 to promote insulin resistance in response to TNF-(alpha) signaling through IKK2. *The Journal of biological chemistry* 283: 35375-35382, 2008.
49. **Zhao L, Kwon MJ, Huang S, Lee JY, Fukase K, Inohara N, and Hwang DH**. Differential modulation of Nods signaling pathways by fatty acids in human colonic epithelial HCT116 cells. *J Biol Chem* 282: 11618-11628, 2007.

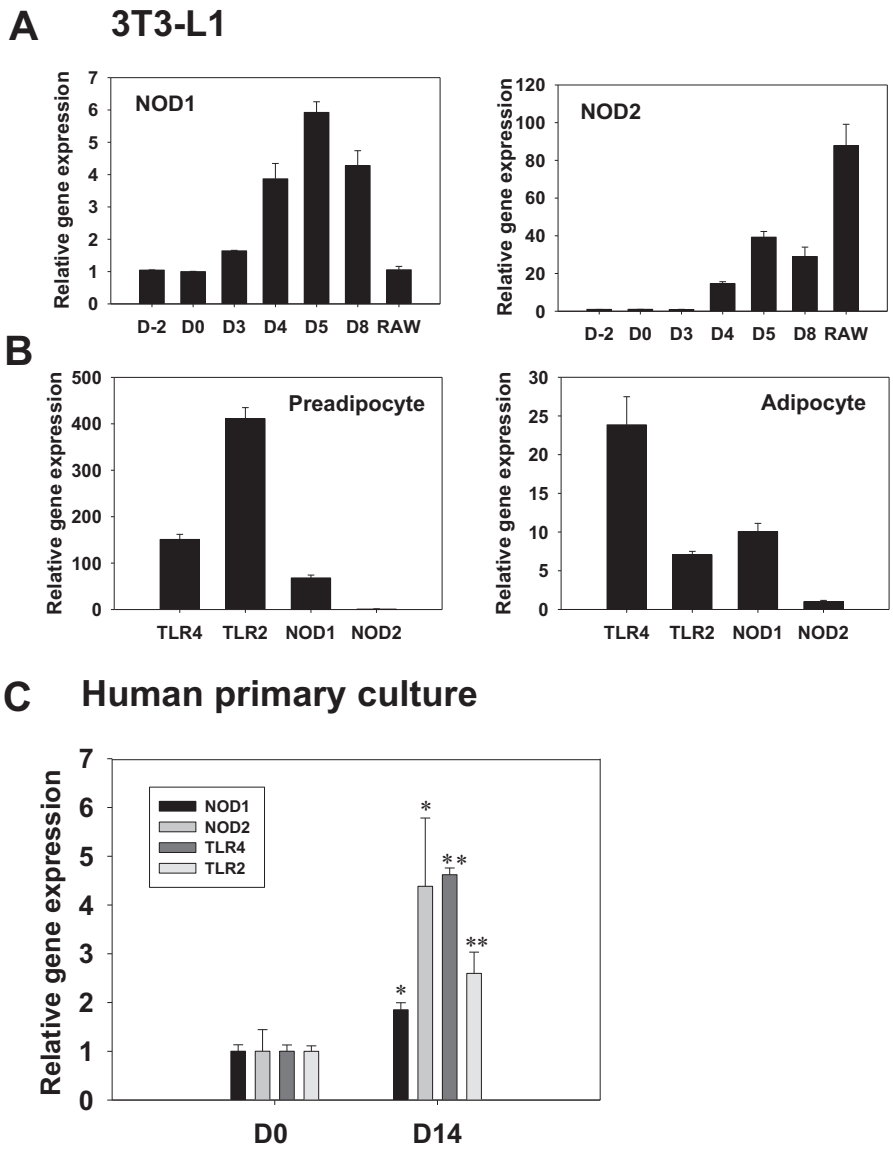
A
3T3-L1
NOD1
Relative gene expression
D-2 D0 D3 D4 D5 D8 RAW
NOD2
B
Preadipocyte
Adipocyte
TLR4 TLR2 NOD1 NOD2
C
Human primary culture
NOD1
NOD2
TLR4
TLR2
D0
D14

Figure 1

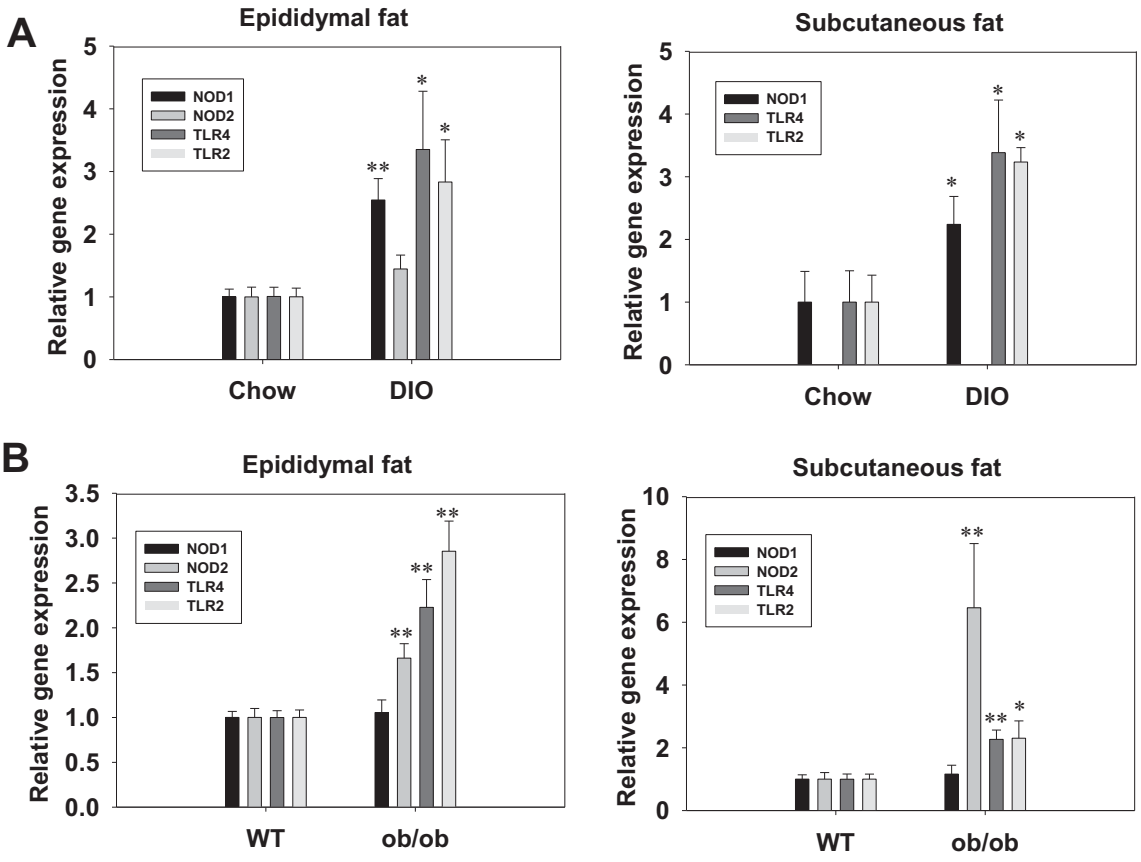
A
Epididymal fat
Relative gene expression
NOD1
NOD2
TLR4
TLR2
Chow
DIO
Subcutaneous fat
B
WT
ob/ob

Figure 2

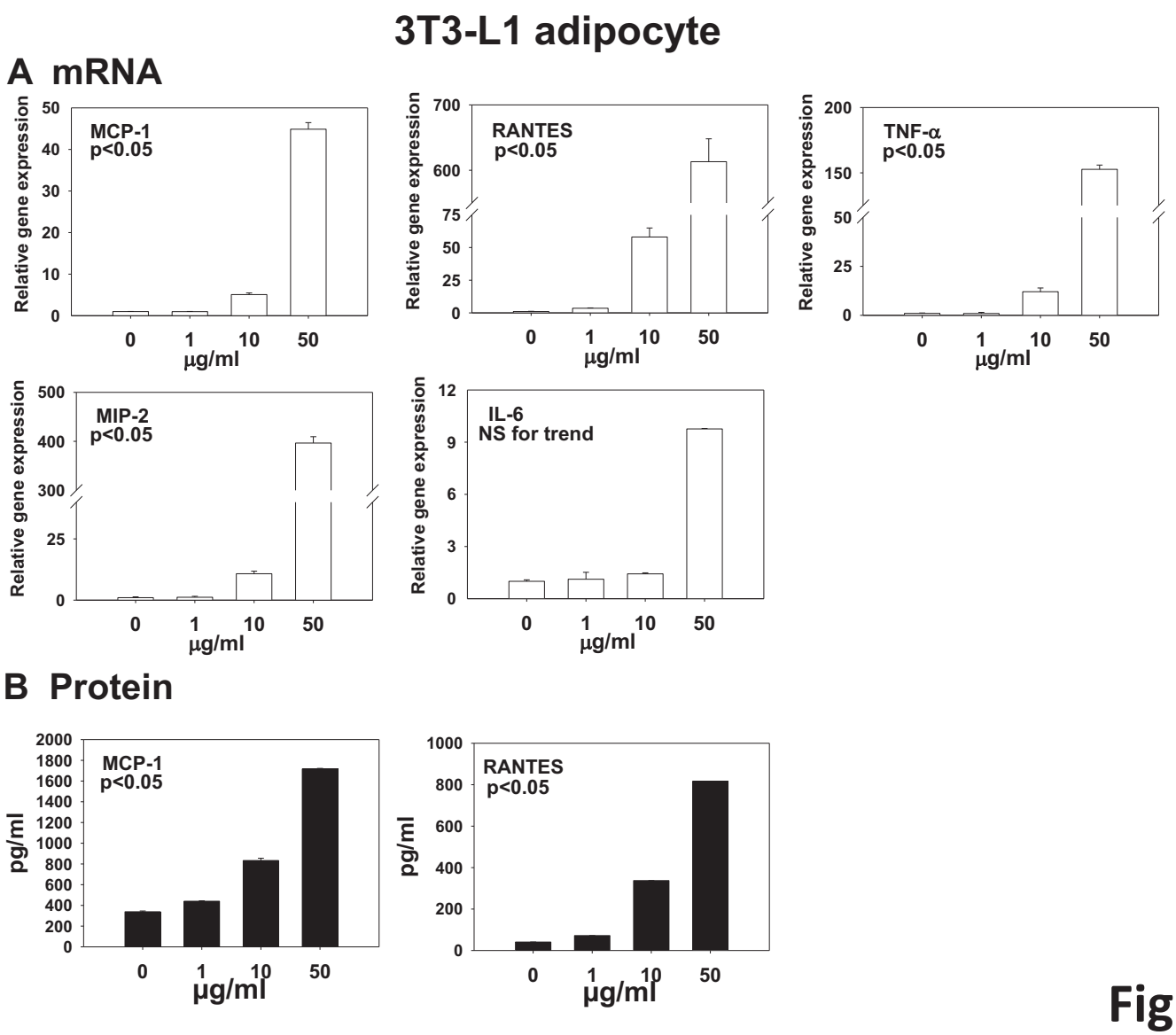
3T3-L1 adipocyte
A mRNA
Relative gene expression
MCP-1
p<0.05
RANTES
p<0.05
TNF-α
p<0.05
MIP-2
p<0.05
IL-6
NS for trend
0 1 10 50
µg/ml
B Protein
pg/ml
MCP-1
p<0.05
RANTES
p<0.05
0 1 10 50
µg/ml

Figure 3

Human primary adipocyte

A Tri-DAP

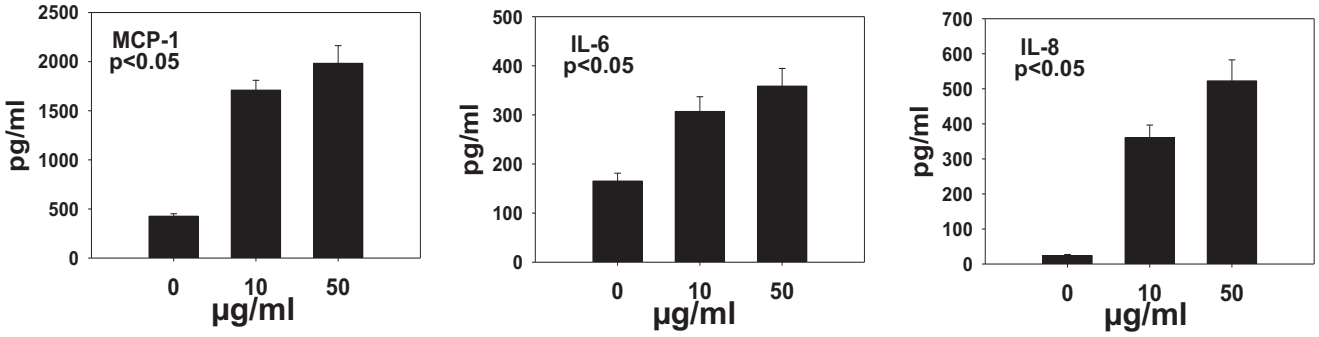

B iE-DAP

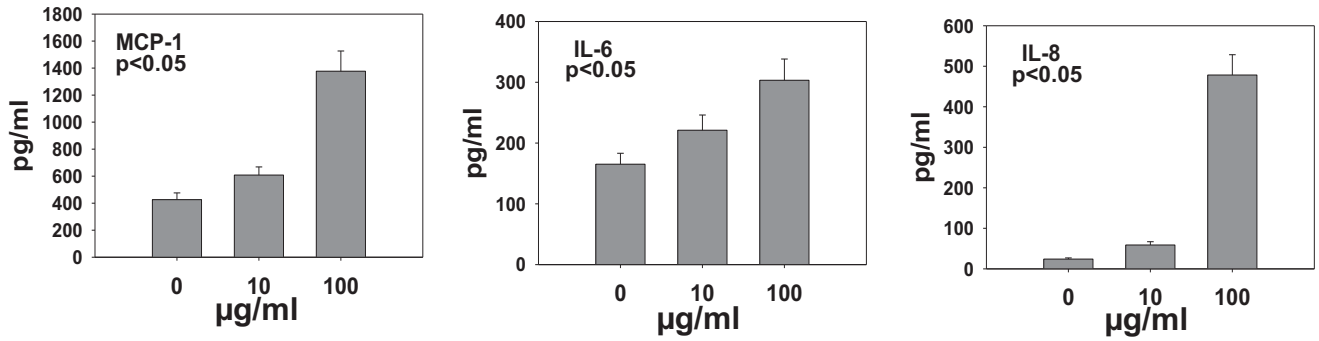

Figure 4

3T3-L1 adipocyte

A mRNA

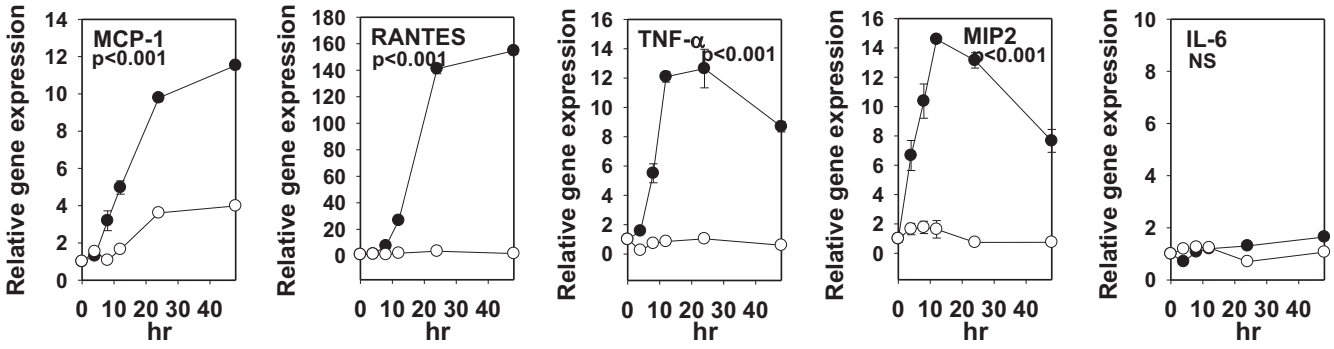

B Protein

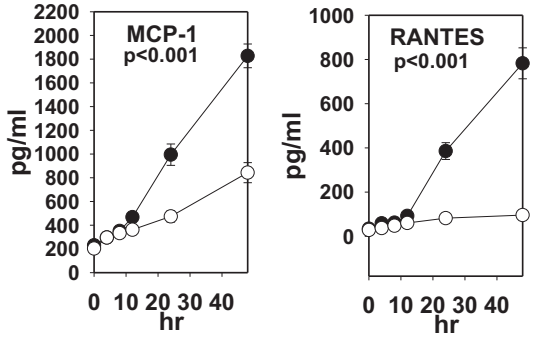

Figure 5

Human primary adipocyte

A mRNA

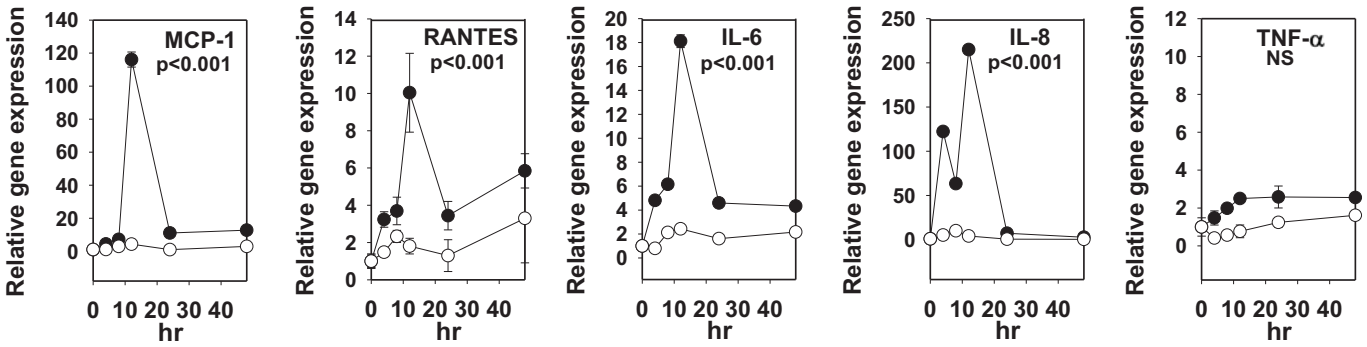

B Protein

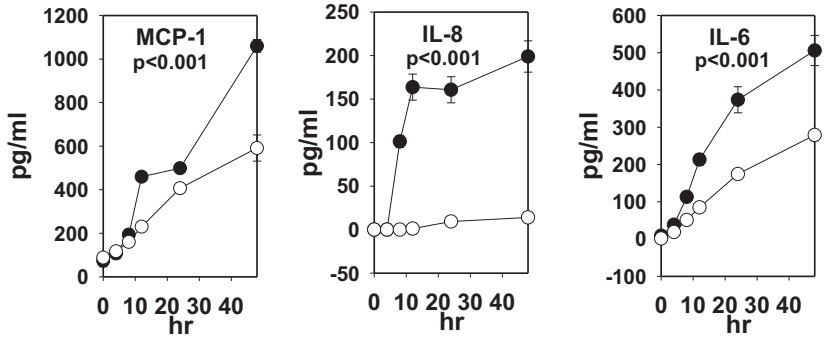

Figure 6

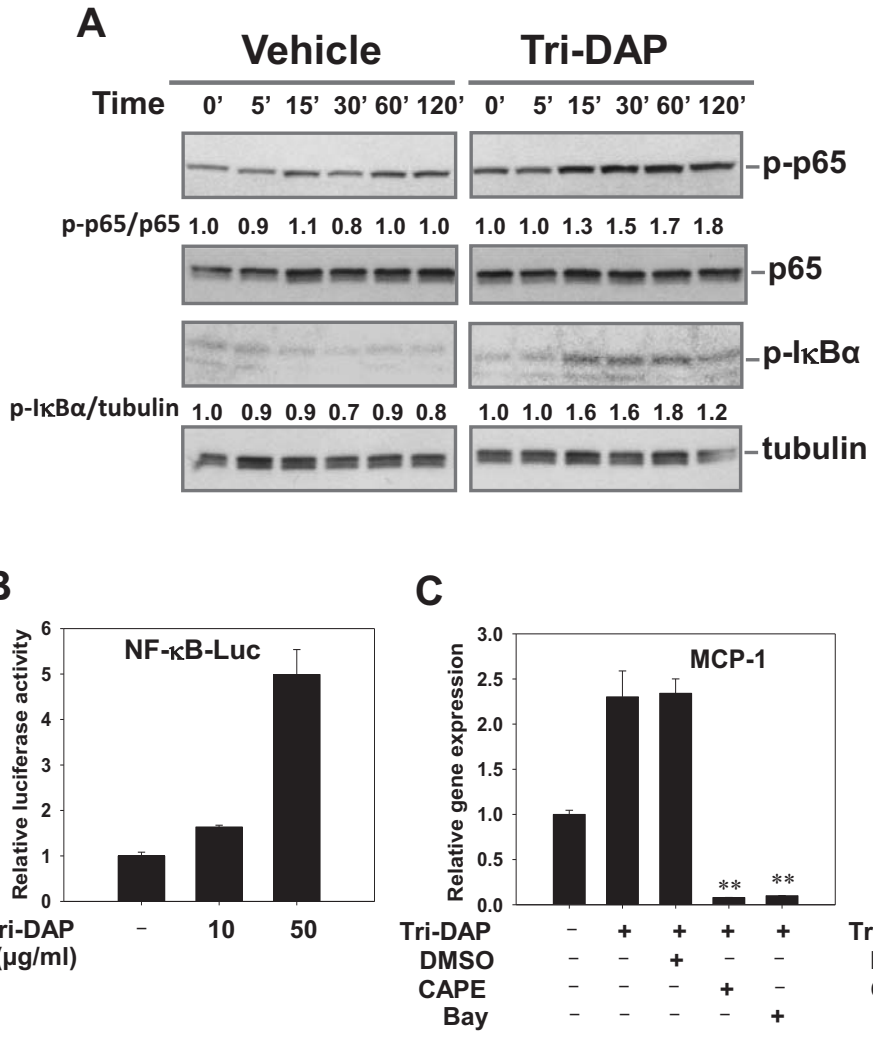
A
Vehicle
Tri-DAP
Time
0' 5' 15' 30' 60' 120' 0' 5' 15' 30' 60' 120'
p-p65
p-p65/p65 1.0 0.9 1.1 0.8 1.0 1.0 1.0 1.0 1.3 1.5 1.7 1.8
p65
p-IκBα
p-IκBα/tubulin 1.0 0.9 0.9 0.7 0.9 0.8 1.0 1.0 1.6 1.6 1.8 1.2
tubulin
B
NF-κB-Luc
Relative luciferase activity
Tri-DAP (μg/ml) − 10 50
C
MCP-1
RANTES
Relative gene expression
Tri-DAP
DMSO
CAPE
Bay
**

Figure 7a

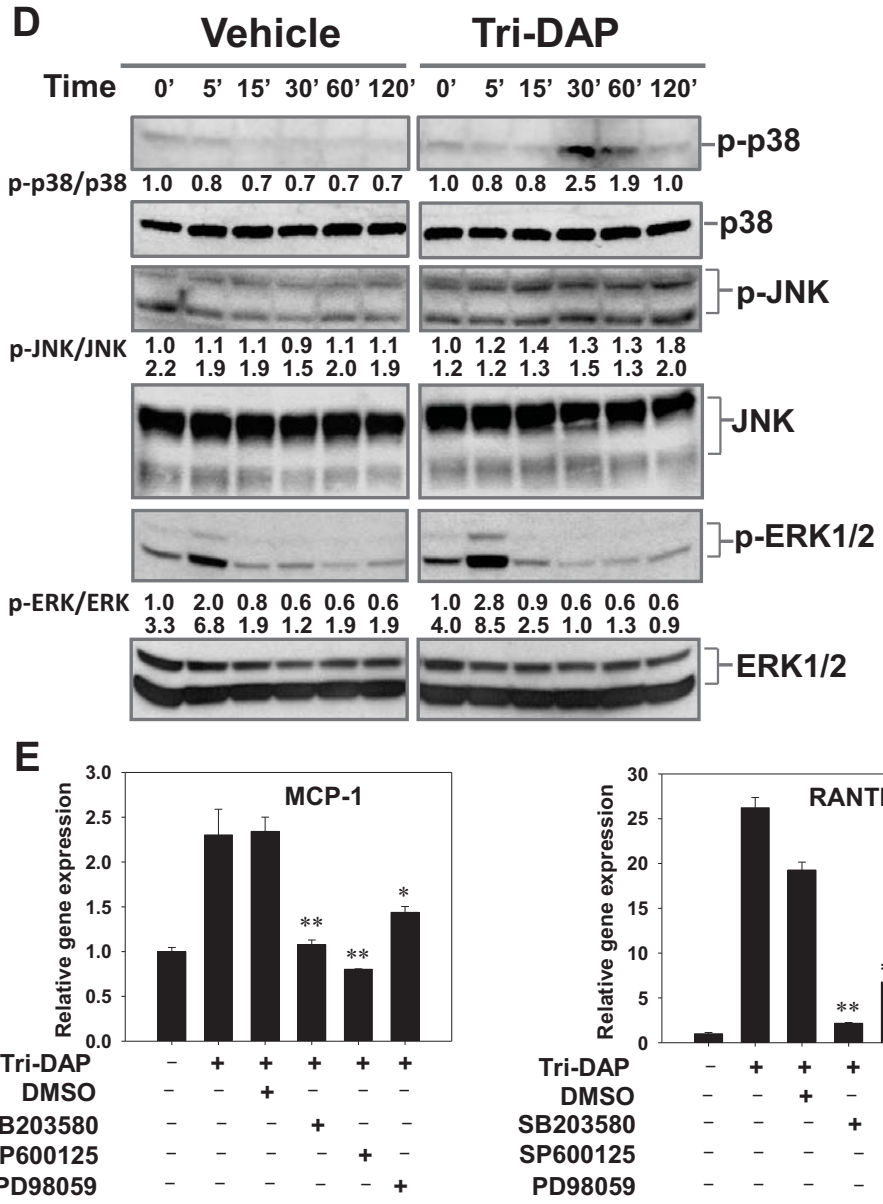
D
Vehicle
Tri-DAP
Time
0' 5' 15' 30' 60' 120' 0' 5' 15' 30' 60' 120'
p-p38
p-p38/p38 1.0 0.8 0.7 0.7 0.7 0.7 1.0 0.8 0.8 2.5 1.9 1.0
p38
p-JNK
p-JNK/JNK 1.0 1.1 1.1 0.9 1.1 1.1 1.0 1.2 1.4 1.3 1.3 1.8
2.2 1.9 1.9 1.5 2.0 1.9 1.2 1.2 1.3 1.5 1.3 2.0
JNK
p-ERK1/2
p-ERK/ERK 1.0 2.0 0.8 0.6 0.6 0.6 1.0 2.8 0.9 0.6 0.6 0.6
3.3 6.8 1.9 1.2 1.9 1.9 4.0 8.5 2.5 1.0 1.3 0.9
ERK1/2
E
MCP-1
Relative gene expression
3.0
2.5
2.0
1.5
1.0
0.5
0.0
**
**
*
Tri-DAP - + + + + +
DMSO - - + - - -
SB203580 - - - + - -
SP600125 - - - - + -
PD98059 - - - - - +
RANTES
Relative gene expression
30
25
20
15
10
5
0
**
**
Tri-DAP - + + + + +
DMSO - - + - - -
SB203580 - - - + - -
SP600125 - - - - + -
PD98059 - - - - - +

Figure 7b

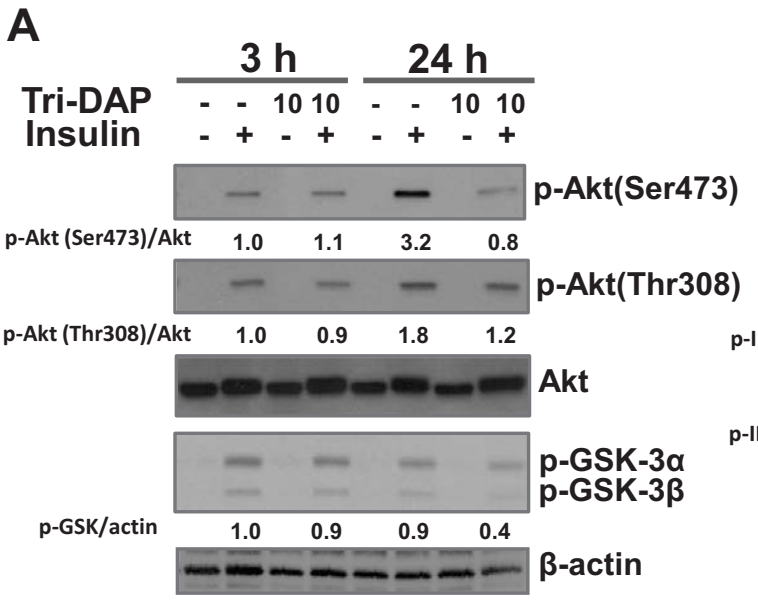
A
3 h
24 h
Tri-DAP
Insulin
- - 10 10 - - 10 10
- + - + - + - +
p-Akt(Ser473)
p-Akt (Ser473)/Akt
1.0 1.1 3.2 0.8
p-Akt(Thr308)
p-Akt (Thr308)/Akt
1.0 0.9 1.8 1.2
Akt
p-GSK-3α
p-GSK-3β
p-GSK/actin
1.0 0.9 0.9 0.4
β-actin

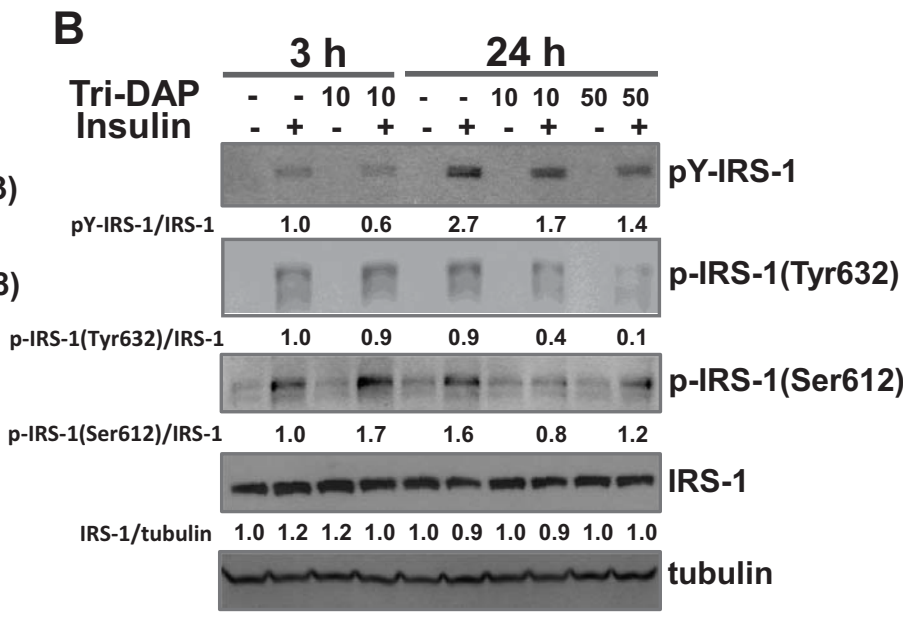
B
3 h
24 h
Tri-DAP
Insulin
- - 10 10 - - 10 10 50 50
- + - + - + - + - +
pY-IRS-1
pY-IRS-1/IRS-1
1.0 0.6 2.7 1.7 1.4
p-IRS-1(Tyr632)
p-IRS-1(Tyr632)/IRS-1
1.0 0.9 0.9 0.4 0.1
p-IRS-1(Ser612)
p-IRS-1(Ser612)/IRS-1
1.0 1.7 1.6 0.8 1.2
IRS-1
IRS-1/tubulin
1.0 1.2 1.2 1.0 1.0 0.9 1.0 0.9 1.0 1.0
tubulin

Figure 8

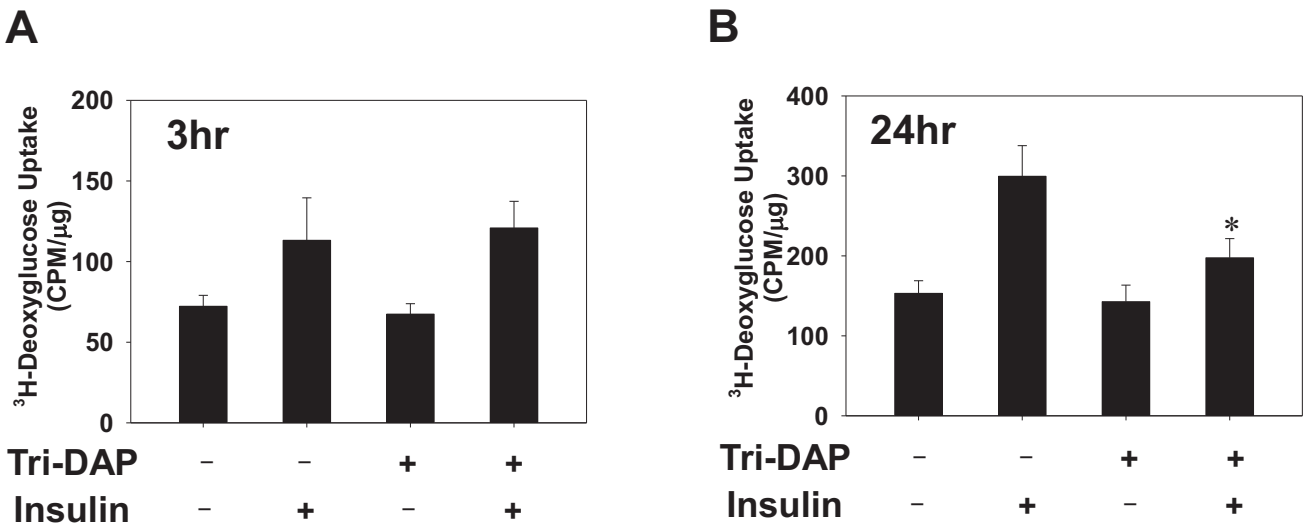
A
3hr
^{3}H-Deoxyglucose Uptake (CPM/μg)
200
150
100
50
0
Tri-DAP – – + +
Insulin – + – +
B
24hr
^{3}H-Deoxyglucose Uptake (CPM/μg)
400
300
200
100
0
*
Tri-DAP – – + +
Insulin – + – +

Figure 9

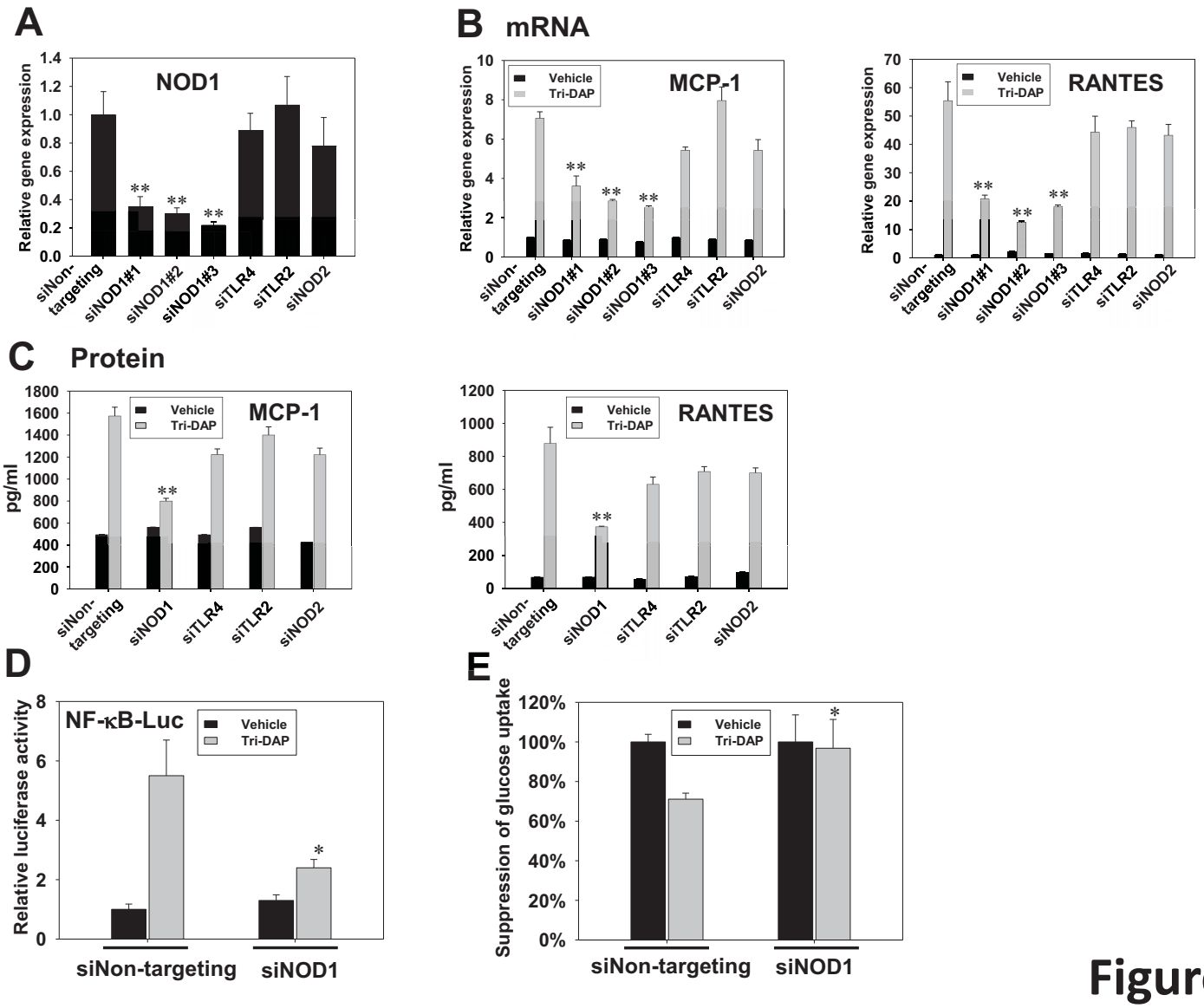
A
NOD1
Relative gene expression
siNon-targeting
siNOD1#1
siNOD1#2
siNOD1#3
siTLR4
siTLR2
siNOD2
B mRNA
MCP-1
RANTES
Vehicle
Tri-DAP
C Protein
pg/ml
siNOD1
D
NF-κB-Luc
Relative luciferase activity
E
Suppression of glucose uptake

Figure 10